Standardization protocol of process efficiencies and activation parameters in heterogeneous photocatalysis: relative photonic efficiencies ζ_r

Nick Serpone [a,*], Geneviève Sauvé [a], Ralf Koch [a], Halima Tahiri [a,b,1], Pierre Pichat [b],
Paola Piccinini [c], Ezio Pelizzetti [c], Hisao Hidaka [d]

[a] Laboratory of Pure and Applied Studies in Catalysis, Environment and Materials, Department of Chemistry and Biochemistry, Concordia University,
Montréal, Que. H3G 1M8, Canada
[b] Laboratoire de Photocatalyse, Catalyse et Environnement, Unité de Recherche associée au CNRS, Ecole Centrale de Lyon, 69131 Ecully Cedex, France
[c] Dipartimento di Chimica Analitica, Università di Torino, 10125 Torino, Italy
[d] Department of Chemistry, Meisei University, 2-1-1 Hodokubo, Hino, Tokyo 191, Japan

Abstract

The quantum yield Φ is crucial in homogeneous photochemistry; in heterogeneous photocatalysis this term remains elusive since the number of absorbed photons remains experimentally difficult to assess. A comprehensive method to standardize and compare process efficiencies in heterogeneous photocatalysis was proposed earlier by describing the relative photonic efficiency ζ_r (J. Photochem. Photobiol., A: Chem., 73 (1993) 11). The method of determining ζ_r is herein tested for the photocatalyzed degradation of phenol as the standard process and Degussa P25 TiO_2 as the standard photocatalyst. The effects of light intensity, reactor geometry, pH, temperature, concentration of reactant and concentration of TiO_2 on ζ_r were examined for the photodegradation of three substituted phenols: 2-methylphenol, 2,4-dimethylphenol and 4-chlorophenol. Relative photonic efficiencies of other phenolic substrates are reported for a given set of conditions. Efficiencies on varying the nature and the source of TiO_2 for the photodegradation of phenol were also explored. These ζ_r are useful to assess process quantum yields once the actual quantum yield for a standard process (Φ_{stand}, for a given photocatalyst and a standard organic substrate) has been rigorously determined; thus $\Phi = \zeta_r \Phi_{stand}$.

Keywords: Heterogeneous photocatalysis; Process efficiencies; Relative photonic efficiencies; Photo-oxidation of phenols; Standardization procedure

1. Introduction

Efficient, environmentally benign and economically feasible processes that lead to mineralization of organic pollutants in drinking waters and in industrial waste effluents are of current interest. Heterogeneous photocatalysis through illumination of aqueous suspensions of TiO_2 offers an advanced oxidation technology capable of purifying waste waters [1]. Titania is a harmless, stable, inexpensive and readily available semiconductor photocatalyst on which complete mineralization of organic substances (phenol, cresols, halogenated aromatics and others) to carbon dioxide and water has been demonstrated [2–7]. What has been lacking, however, is a general method of comparing process efficiencies. Methods that assess process efficiency in an industrial

environment such as "electric energy per order" [8] and "energetic efficiency of degradation" [9] have been proposed. While these are useful to compare the economics of different industrial strategies, they fail to provide a relatively simple method to establish photo efficiencies [10]. Vogler and coworkers [11] recommended the usage of formal rate constants in the photodegradation of various organics as a measure of the efficiency of photo-oxidations.

Too often, the heterogeneous photocatalysis literature uses the term quantum yield which it has defined as the number of molecules converted relative to the total number of photons incident on the reactor walls, for a sometimes ill-defined reactor geometry and for a large spectral irradiation window (polychromatic radiation), rather than the number of absorbed quanta at a given wavelength to satisfy the photochemical definition of Φ in homogeneous phase [12,13]. In the latter phase, the overall quantum yield $\Phi_{overall}$ expresses the number N_{mol} of molecules undergoing an event (conversion of reactants or formation of products) relative to the

---

* Corresponding author.
[1] Doctoral Stagiaire from the Ecole Centrale de Lyon, Ecully, France, 1994–1995.

number N_{ph} of quanta absorbed by the reactant(s) or by the photocatalyst [12]:

$$\Phi_{overall} = \frac{N_{mol}/cm^{3-}\ s}{N_{ph}/cm^{3-}\ s}$$

$$= \frac{\text{rate of reaction}}{\text{rate of absorption of radiation}} \quad (1)$$

Analogous descriptions have been proposed for heterogeneous systems [13–15]. No particular difficulties are encountered for a homogeneous system. In heterogeneous media the relationship in Eq. (1) has been extended, modified and applied in analogous fashion [16–19]. Because the number N_{ph} of absorbed photons is experimentally difficult to access owing to reflection, scattering (see below), transmission (for transparent colloidal sols) and absorption by the suspended particulates, usage of the term quantum yield as defined in terms of incident photons in the heterogeneous photochemical literature has led to a high degree of confusion. Some suggested methods to determine N_{ph} have appeared [17–20].

Complicating the measurements of the number (or rate) of absorbed quanta by a semiconductor photocatalyst is most markedly the significant extent of light scattered by the particulate matter in a dispersion which could reach, according to some accounts, 13–76% of the total incident photon flux [17]. A metal oxide material such as TiO_2 particulates (anatase or rutile) can never absorb all the incident photon flux from a given source [10] as the intensity I of scattered light depends on the refractive indices as

$$\frac{I}{I_0} = (\text{constant}) \frac{\eta_1}{\eta_0} \quad (2)$$

where I_0 is the incident light, η_0 is the refractive index of the medium and η_1 is the refractive index of the photocatalyst (in this case) [21]. When $\eta_1 \approx \eta_0$, the extent of scattered light is negligible whereas, for $\eta_1 > \eta_0$ the light is highly scattered. For the materials making up the photocatalytic system under examination, $\eta_0 = 1.33$ for water, $\eta_1 = 1.5$–1.7 for glass, $\eta_1 = 3.87$ for rutile TiO_2 and $\eta_1 \approx 2.5$–3 for anatase TiO_2 at 365 nm radiation [22,23]. The number of photons absorbable by TiO_2 seems to be about 60–65% [22,24].

Additional considerations suggest that the photochemically defined quantum yield will be difficult to describe experimentally [20] (however, see [24] for a possible solution). Consequently, the reported "quantum yields" have sometimes been reported as lower limits not allowing for scattered light [15]. In defining Eq. (1), we must recognize that semiconductor-assisted photo-oxidations take place on the solid catalyst (see below), and thus the catalytic properties of the catalyst surface are not negligible, as the course of the reactions depends highly on the characteristics of the surface after light activation. For example, usage of two TiO_2 photocatalysts obtained from different sources, or from different batches from the same source, may give different intermediate products or give different distributions of intermediates for experiments carried out under otherwise identical condi-

tions. In this regard note the variations in intermediates between Degussa P25 titania and a TiO_2 sample from Sargent–Welch (see below and Figs. 2–4). This calls attention to the necessity of reporting the characteristics of the photocatalyst [15,16,19]. Moreover, a distinction should be made between the light-activated steps, which are related to the quantum yield, and the ensuing catalytic steps in the photocatalyzed process, which depend highly on the surface properties of each photocatalyst.

In heterogeneous photocatalysis, the numerator in Eq. 1 expresses the rate of a catalyzed heterogeneous reaction which is related to the number of catalytically surface active sites [16]; unfortunately, these are also not experimentally attainable [25]. To bypass this difficulty, the number of active sites is often replaced [26] by (i) the surface area of the catalyst, (ii) the mass of the catalyst or (iii) by the number of surface OH groups on a photocatalyst such as TiO_2 [17–19]. Regrettably, none of these suggestions describes the actual heterogeneous rate since measuring the surface area for a somewhat porous catalyst (for example) comprises both the external and the internal surface areas [20]; for various reasons the latter may not be useful in some catalytic events. Also, not all the surface sites occupied by OH groups are necessarily catalytically active [25] especially since there are different kinds of OH group. Also, depending on the reactor geometry, agglomeration and stirring, all the calculated catalyst surface (Brunower–Emmett–Teller measurements in the dry state) may not be accessible to the substrate being converted.

A simple means of assessing process efficiencies for equal absorption of photons is therefore desirable in heterogeneous photocatalysis. The initial photoconversion of phenol was herein chosen as the standard process and Degussa P-25 titania, a material used extensively, as the standard photocatalyst. The choice of phenol was dictated by the recognition that the molecular structure of phenol is present in many organic pollutants and, like many of these, is degraded essentially by oxidation rather than reduction.

Because of several inherent difficulties, the expression relative photonic efficiency ζ_r was retained earlier [10,25] and was described in terms of the number of incident photons. The method described affords comparison of process efficiencies and avoids the confusion in the literature with quantum yields.

The objective of this paper, therefore, focuses on a method that standardizes process efficiencies of degradation of various organic substrates for a given set of conditions. The method circumvents the inherent difficulties encountered in the precise evaluation of the number of quanta absorbed by the photocatalyst (titania), difficulties with utilization of different light sources, different reactor geometries and other unspecified factors by referring all the results to an equivalent experiment carried out for a standard process. Note that the proposed method does not yield "absolute values" of the photon efficiencies. However, these ζ_r can at a later date be converted into the photochemically defined Φ once a proto-

col(s) or method is found that gives the precise description of the number of absorbed quanta, and thereby a quantum yield Φ_{stand} for a given photocatalyst and a given substrate; whence, $\Phi = \zeta_r \Phi_{stand}$. Recent laser work from our laboratory suggests that Φ cannot be greater than about 10% for TiO$_2$ photocatalysts [27].

An important observation about Eq. (1) is that, since the numerator also expresses the "rate of reaction", the overall quantum yield depends on the reactant concentration. As correctly noted by Braun et al. [13] and re-emphasized more recently by Cassano and coworkers [20], only for a zero-order reaction is the overall quantum yield uniquely defined at a given wavelength. In homogeneous photochemistry, the problem is normally overcome by determining Φ at small conversions (less than about 10%) of reactants, a point not often respected in heterogeneous photocatalysis where the focus is complete mineralization (100% transformation) of the substrate, at least in studies of environmental interest that aim at the elimination of organic pollutants in water.

The efficiencies ζ_r reported here refer specifically to substrate disappearance. The present report extends the earlier work [10] and demonstrates the general applicability of the proposed method of ζ_r. The effects of light intensity, reactor geometry, pH, temperature, concentration of reactant and concentration of TiO$_2$ on ζ_r were examined for three phenolic substrates: 2-methylphenol (2-MePhOH), 2,4-dimethylphenol (2,4-Me$_2$PhOH) and 4-chlorophenol (4-ClPhOH). Additionally, ζ_r of other organic substrates were determined at some specified conditions. The effects of the nature and the source of various TiO$_2$ specimens on ζ_r were also explored.

2. Experimental section

2.1. Materials

The following phenol derivatives were Aldrich chemicals (purity, greater than 99%) and were used without further treatment: phenol, pyrocatechol, hydroquinone, 2-methylphenol, 3-methylphenol, 4-methylphenol, 2-chlorophenol, 3-chlorophenol, 4-chlorophenol, 2,4-dichlorophenol, 2,3-dimethylphenol, 2,4-dimethylphenol, 2,5-dimethylphenol, 2,6-dimethylphenol, 3,4-dimethylphenol, 3,5-dimethylphenol, and 2,3,5-trimethylphenol. The TiO$_2$ samples were from Degussa P25 (batch A, batch B and an unknown batch C), Sargent–Welch (log 6G17B), Tioxide (AHR T CS 16986), Baker & Adamson (batch WO36) and Fluka AG (CH-9470 Buch batch 236189 284. The solvents used throughout were methanol (BDH, Omnisolv grade) and doubly distilled water, unless noted otherwise.

2.2. Methods and procedures

Photodegradation reactions were performed using the following procedure. The aqueous reactant solutions (50 ml)

were adjusted to pH 3.0 using HCl prior to addition of 0.100 g of Degussa P25-A titania (2.0 g l^{-1}). The reactor was an unstoppered 50 ml bottle. The mixture was magnetically stirred in the dark for several minutes to pre-equilibrate the quantities of both oxygen and substrate between the TiO$_2$ particles and the bulk solution, subsequent to which it was exposed to light. About 1 ml aliquot of the suspension was taken at various time intervals and vacuum filtered through a MSI 25 mm nylon membrane (0.22 μm) prior to analysis.

The light source was a 1000 W Hg–Xe lamp operated at 825 W and equipped with a water jacket to filter out IR radiation. This set-up gave a power density of about 190 mW cm^{-2} at the window of the reactor, measured with a Coherent Radiation 210 power meter. Unless specified otherwise, the temperature was ambient and broad-band irradiation was used. This experimental simplification was possible because the relative photonic efficiency of phenol showed no variations when using either monochromatic incident radiation (365 $\pm$ 10 nm) or broad-band simulated sunlight radiation [10]. Wavelengths below 300 nm were cut off by the Pyrex glass reactor, thus eliminating direct photolysis of the organic substrates, at least in acidic media.

The effects of altering various parameters on relative photonic efficiencies were examined for 2-dimethylphenol, 2,4-dimethylphenol and 4-chlorophenol against phenol as the standard probe. Initial reactant concentrations were about 20 mg l^{-1}: [phenol]$_i \approx 200$ μmol l^{-1}, [2-MePhOH]$_i \approx 185$ μmol l^{-1}, [2.4-Me$_2$PhOH]$_i \approx 160$ μmol l^{-1} and [4-ClPhOH]$_i \approx 156$ μmol l^{-1}. Appropriate neutral density filters were used to assess the effect of light intensity variations. The effect of reactor geometry was probed using a bottle, a round-bottomed flask and a cell with flat parallel windows; they could hold a 50 ml solution. pH effects were examined by taking the aqueous solution at pH 3.0 and adjusting it to pH 4.0, 5.0 and 6.0 with NaOH. A water-jacketed reactor was employed to investigate the effect of temperature (± 0.5 °C) on the photodegradations at 12.0, 31.0, 48.0 and 67.5 °C. The effect of the TiO$_2$ concentration was examined at [TiO$_2$] = 0.2, 0.5 and 1 g l^{-1} (in addition to 2 g l^{-1}), while the influence of the initial concentration of organic substrate was examined by diluting an approximately 1 mmol l^{-1} solution with pH 3.0 distilled water (HCl); the resulting concentrations were 40, 120, 200, 250, 400 and 800 μmol l^{-1}.

The relative photonic efficiencies of other phenols were also determined for an initial reactant concentration of about 200 μmol l^{-1}, at pH 3 and ambient temperature. ζ_r was also assessed for various titania photocatalyst specimens from different sources and various batches of Degussa P25 TiO$_2$; [phenol]$_i \approx 200$ μmol l^{-1}.

2.3. Analyses

The rate of substrate disappearance was monitored by high performance liquid chromatography (HPLC) using a Waters Associates liquid chromatograph equipped with a 501 HPLC pump, a 441 absorbance detector and a Hewlett–Packard
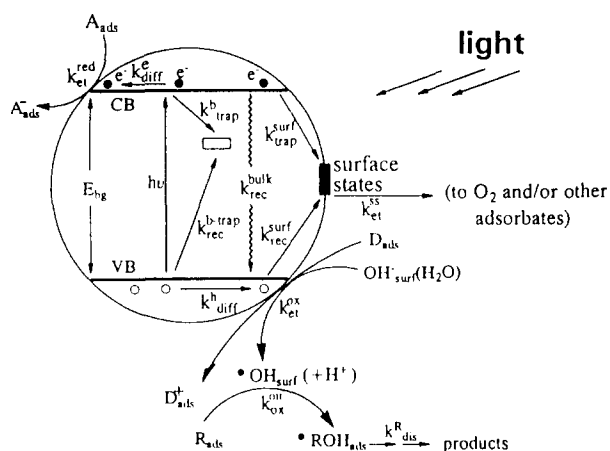
Fig. 1. Cartoon illustrating some of (but not all) the photophysical and photochemical processes in a semiconductor cluster [28].

3396A integrator. The analytical conditions were as follows: column, μ BONDAPAK™ C_{18}, 3.9 × 300 mm; column temperature, ambient; flow rate, 2.0 ml min^{-1}; mobile phase, 50:50 (v/v) methanol:water; detector, absorbance detector; $\lambda = 214$ nm (zinc lamp), threshold; recorder sensitivity, 0.1 (0.5 for [cpd]$_i$ < 150 μmol l^{-1}, 0.2 for [cpd]$_i$ = 250 and 400 μmol l^{-1}, and 0.5 for [cpd]$_i$ = 800 μmol l^{-1}).

3. Results and discussion

3.1. Heterogeneous photocatalytic steps

We begin by recalling the variety and complexity of events that take place when an aqueous solution containing a phenol is irradiated in the presence of TiO$_2$ (Fig. 1) [28]. When photons of energy equal to or exceeding the band gap energy of titania (anatase, 3.2 eV band gap) are absorbed, valence band (VB) electrons are promoted to the conduction band (CB). The fates of an e_{cb}^- are multiple. It may recombine in the bulk with h_{vb}^+ (k_{rec}^{bulk}), may diffuse to the particle surface (k_{diff}^e) and can reduce adsorbed molecules (k_{et}^{red}). It may also be trapped on the surface (k_{trap}^{surf}) and in the bulk (k_{trap}^b). The destiny of a h_{vb}^+ is similar; at the surface it can oxidize an adsorbed molecule. Free or trapped electrons and holes rapidly recombine in the bulk and at the surface. These events are only the "tip of the iceberg" as the particles are fraught with several bulk and surface traps for e_{cb}^- and h_{vb}^+ and a number of other unknown defects, each of which embodies trapping and detrapping events that will indeed influence the overall quantum yield of formation of the entity ultimately responsible for initiation of the oxidative photodegradation of organic compounds (e.g. phenol) at the semiconductor surface: VB hole or the surface-trapped hole, ≡Ti–'OH. Recent reports [27,29] suggest the latter species is formed in subpicosecond time (about 200 fs).

Two general mechanisms for photomineralizations to CO$_2$ are currently being debated: (i) the photogenerated holes oxidize adsorbed phenol directly according to

$$D_{ads} + h_{VB}^+ \longrightarrow D_{ads}^+ \qquad (3)$$

or (ii) they first oxidize adsorbed water or OH$^-$ groups to give the ≡Ti–'OH radical:

$$\equiv Ti-OH_{surf}^- \text{ (or } H_2O) + h_{VB}^+ \longrightarrow$$
$$\equiv Ti-'OH_{surf}(\text{and } H^+) \qquad (4)$$
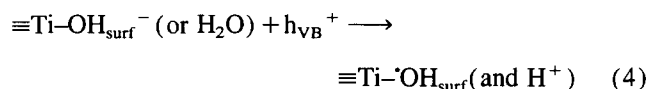
In turn, the hydroxyl radical oxidizes adsorbed phenol to yield hydroxylated radical intermediates, e.g. hydroquinone, pyrocatechol and others [30]. Subsequently, these react further to yield the final products CO$_2$ and H$_2$O. Note that the intermediates evoked in mechanism (ii) may also result from mechanism (i) if oxidized phenol (a cation) reacted with water [31,32]. A detailed discussion on the mechanisms may be found elsewhere [25].

Photo-oxidations of organic compounds seldom, if ever, occur in the absence of oxygen. Pre-adsorbed O$_2$ is readily reduced to yield the superoxide radical anion O$_{2(ads)}^{\cdot-}$ and further reduction gives the peroxide dianion O$_{2(ads)}^{2-}$. Consequently, surface-trapped electrons that would otherwise quickly recombine with trapped holes are removed, thereby enhancing the anodic surface reactions.

The above considerations infer that any attempt at describing the actual quantum yield of any of the processes in Fig. 1 must account for all the events in Fig. 1. The simple method of ζ_r proposed circumvents the need for such descriptions and permits comparison of process efficiencies relative to some acceptable standard.

3.2. Photo-oxidations

Fig. 2 shows typical HPLC chromatograms obtained under otherwise identical conditions; they illustrate the temporal course of the photodegradation of phenol, 2-methylphenol, 4-chlorophenol and 2,4-dimethylphenol. Four-point linear fit calibration curves were utilized to quantify the compounds. The signal at 1.1 min was present in all chromatograms, including a water blank, and is therefore attributed to the mobile phase. The peak eluting at 2.6 min is that of phenol; it decreased with irradiation time from $t = 0$ (curve (a)) to $t = 25$ min (curve (d)). The appearance of a small peak at 1.6 min is that of hydroquinone (1,4-dihydroxybenzene). 2-Methylphenol eluted at 3.7 min while 4-chlorophenol eluted at 4.9 min and 2,4-dimethylphenol at 5.8 min.

The photodegradation of phenol was also performed using irradiated Sargent–Welch TiO$_2$ suspensions (Fig. 3). The chromatograms were more complex than those shown in Fig. 2 with Degussa P25 TiO$_2$. The features at 1.6 min and 2.0 min are hydroquinone and pyrocatechol (1,2-dihydroxybenzene) respectively. Identification was confirmed from chromatograms of the pure compounds.

A comparison between the temporal course of the photodegradation of phenol in the presence of Degussa P25 TiO$_2$ and Sargent–Welch TiO$_2$ is illustrated in greater detail in Fig. 4. The two profiles obtained are significantly different. Phenol disappeared faster in the presence of irradiated Sargent–
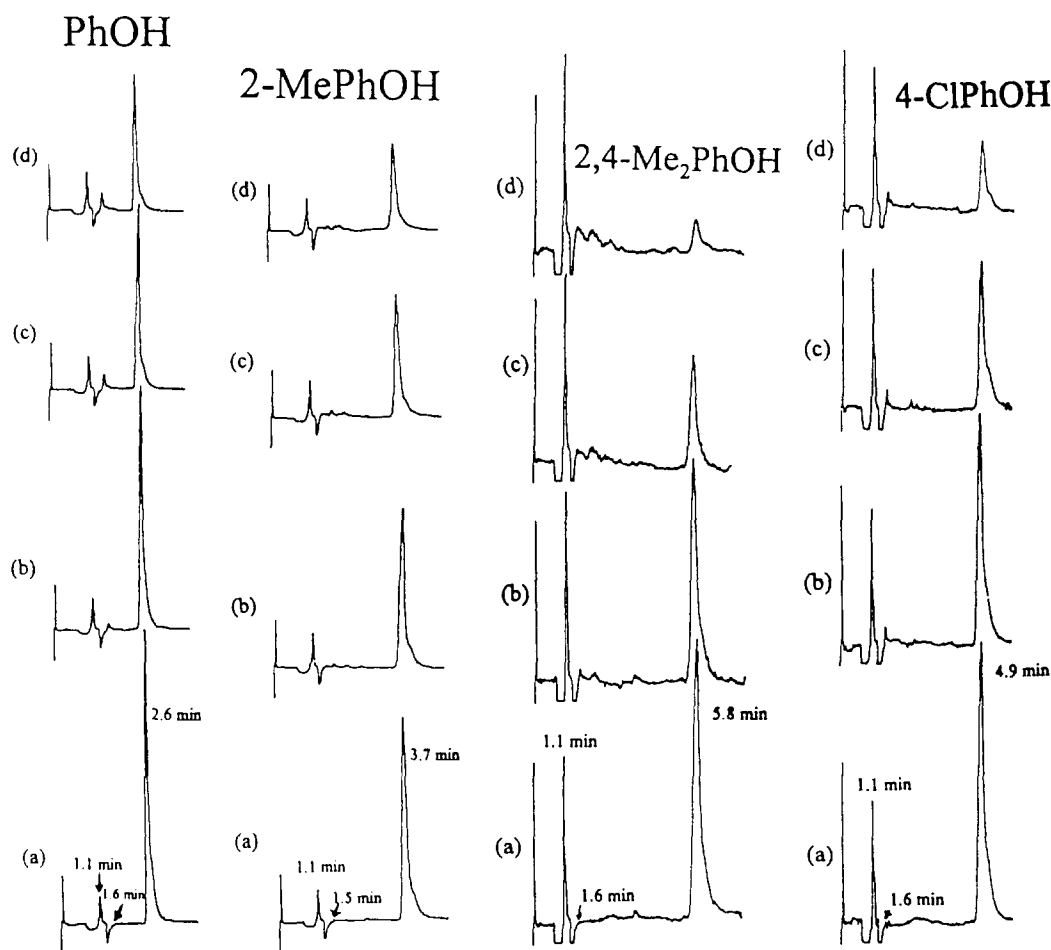
Fig. 2. HPLC chromatograms showing the changes in concentration of substrate as a function of irradiation time for the photodegradation of phenol, 2-methylphenol, 2,4-dimethylphenol and 4-chlorophenol in the presence of irradiated TiO_2, for the following irradiation times for (reactor, 50 ml bottle; $[TiO_2] = 2$ g l^{-1}; [substrate]$_i \approx 20$ mg l^{-1}; pH 3.0): phenol: curve (a), 0 min; curve (b), 5 min; curve (c), 15 min; curve (d), 25 min; irradiation times for 2-MePhOH: curve (a), 0 min; curve (b), 6 min; curve (c), 15 min; curve (d), 25 min; irradiation times for 2,4-Me$_2$PhOH: curve (a), 0 min; curve (b), 3.5 min; curve (c), 9 min; curve (d), 17 min; irradiation times for 4-ClPhOH: curve (a), 0 min; curve (b), 5 min; curve (c), 15.5 min; curve (d), 25.5 min. The feature at 1.1 min is due to the elution of the solvent (water–methanol) and any compounds not retained by the column.

Welch TiO_2 than in an illuminated Degussa P25 titania suspension. A larger number of intermediates (and in greater quantities) were detected in the former suspensions. This calls immediate attention to obvious variations in the surface properties of the two different titania specimens.

Phenol photodegradations on irradiated Sargent–Welch, Tioxide and Fluka TiO_2 suspensions were comparable. Photodegradations with Baker & Adamson TiO_2 were slower. Except for Degussa P25 titania, of the intermediates detected under the prevalent but identical conditions with the other specimens, pyrocatechol formed in greatest quantity, followed by hydroquinone and probably by (unidentified) intermediate 1. The latter may be the 4-chlorocatechol species identified by others [32,33].

3.2.1. Effect of pH.

pH changes strongly affect the photocatalyst surface characteristics since titania possesses both acidic and basic properties; the point of zero charge is about 6 [34–36]. The surface is positively charged at pH below about 6 and nega-

tively charged above pH about 6. In most cases, photo-oxidations were carried out at pH about 3, also to minimize direct photolysis known to occur significantly in alkaline media [37].

Photo-oxidation of phenol and 2-methylphenol were slower at pH 3 and about the same at pH 4, 5 and 6; for 2,4-dimethylphenol and 4-chlorophenol, the temporal course of the photodegradation was similar at all the pH values examined. Initial rates increased slightly with pH for the four phenolic substrates (Fig. 5) and confirm earlier results with 3,4-dimethylphenol [34] and with findings on 4-chlorophenol [38]. Photodegradations at pH > 6 were not examined; Terzian [34a] and Terzian and Serpone [34b] found little variations in the first-order rate constants for the photodegradation of 3,4-dimethylphenol at pH 5–10.

3.2.2. Effect of initial concentration of substrate

Plots of normalized concentrations vs. irradiation time for the phenolic substrates at five initial concentrations (40, 120, 250, 400 and 800 μmol l^{-1}) are reported in Fig. 6. The initial
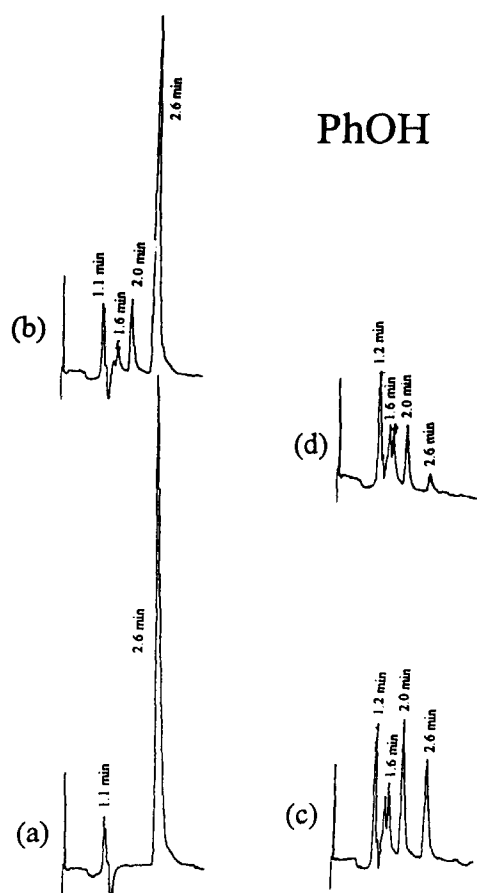
PhOH

(b)

(d)

(a)

(c)

Fig. 3. HPLC chromatograms showing the changes in concentration of phenol and intermediates as a function of irradiation time for the photodegradation of phenol in the presence of irradiated Sargent–Welch TiO_2 for the following irradiation times (reactor, 50 ml bottle; $[TiO_2] = 2$ g l^{-1}; [phenol]$_i \approx 200$ μmol l^{-1}; pH 3.0): curve (a), 0 min; curve (b), 6 min; curve (c), 22.3 min; curve (d) 44.5 min. The feature at 1.1 min is due to the elution of the solvent (water–methanol); the peaks at 1.6, 2.0 and 2.6 are due to hydroquinone, pyrocatechol and phenol respectively; the peak at 1.5 min is probably chlorocatechol (see text).

rates of the photocatalyzed reactions could be fitted to a simple rate expression for saturation-type kinetics:

$$R_{initial} = \frac{k_{obs}K_{ads}[substrate]_i}{1 + K_{ads}[substrate]_i}$$ (5)

where k_{obs} is the observed rate constant and K_{ads} is the adsorption coefficient of the phenol on the photocatalyst's surface. Fig. 7 displays plots of initial rate vs. initial concentrations for phenol, 2-methylphenol, 2,4-dimethylphenol and 4-chlorophenol. The full curves were drawn for the various values of k_{obs} and K_{ads} noted in Fig. 7. For 4-chlorophenol, K_{ads} is $1.3 \pm 0.2 \times 10^4$ M^{-1}, a value in accord with that (1.66×10^4 M^{-1}) reported by Al-Sayyed et al. [38]. The surface coverage for this chlorophenol extends from about 30 to about 90% in the concentration range from 40 to 800 μmol l^{-1}. Adsorption of the substrates on Degussa P25 titania particles varies as 2,4-Me$_2$PhOH $\approx$ PhOH $<$ 4-ClPhOH $\leqslant$ 2-MePhOH.

3.2.3. Effect of light intensity

The rates of photocatalyzed oxidation of organics scale with I at low intensities and scale with $I^{1/2}$ at higher intensities; at yet higher intensities, mass transfer limitations come
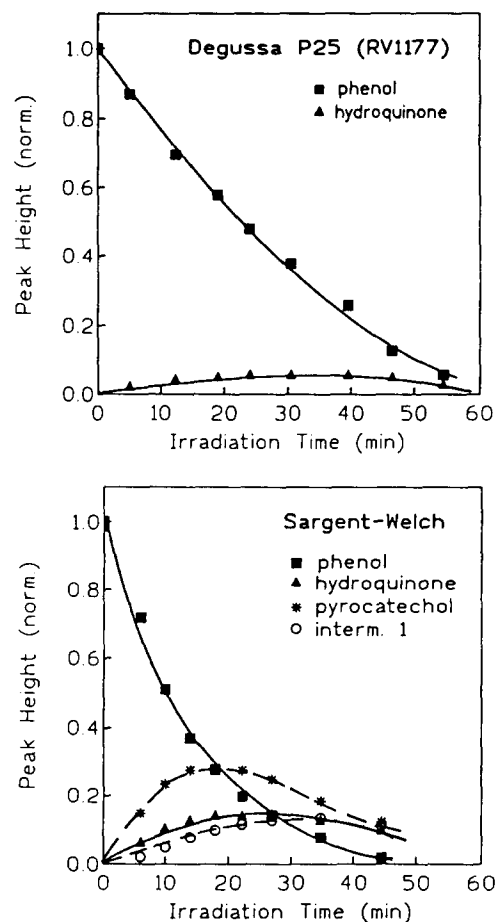
Fig. 4. Plots of normalized peak heights as a function of irradiation time showing the photodegradation of phenol and the formation and decomposition of detected intermediates when irradiated in the presence of TiO_2 (2 g l^{-1}) from Degussa P25 and Sargent–Welch (reactor, 50 ml bottle; [phenol]$_i \approx 200$ μmol l^{-1}; pH 3.0). Experiments were run under otherwise identical conditions.
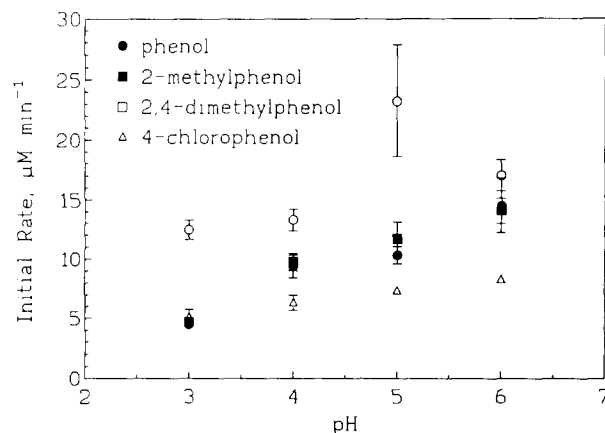
Fig. 5. Plots of initial rate vs. pH showing the effect of initial pH on the photodegradation of 2-methylphenol, 2,4-dimethylphenol and 4-chlorophenol (reactor, 50 ml bottle; $[TiO_2] = 2$ g l^{-1}; [substrate]$_i \approx 20$ mg l^{-1}).
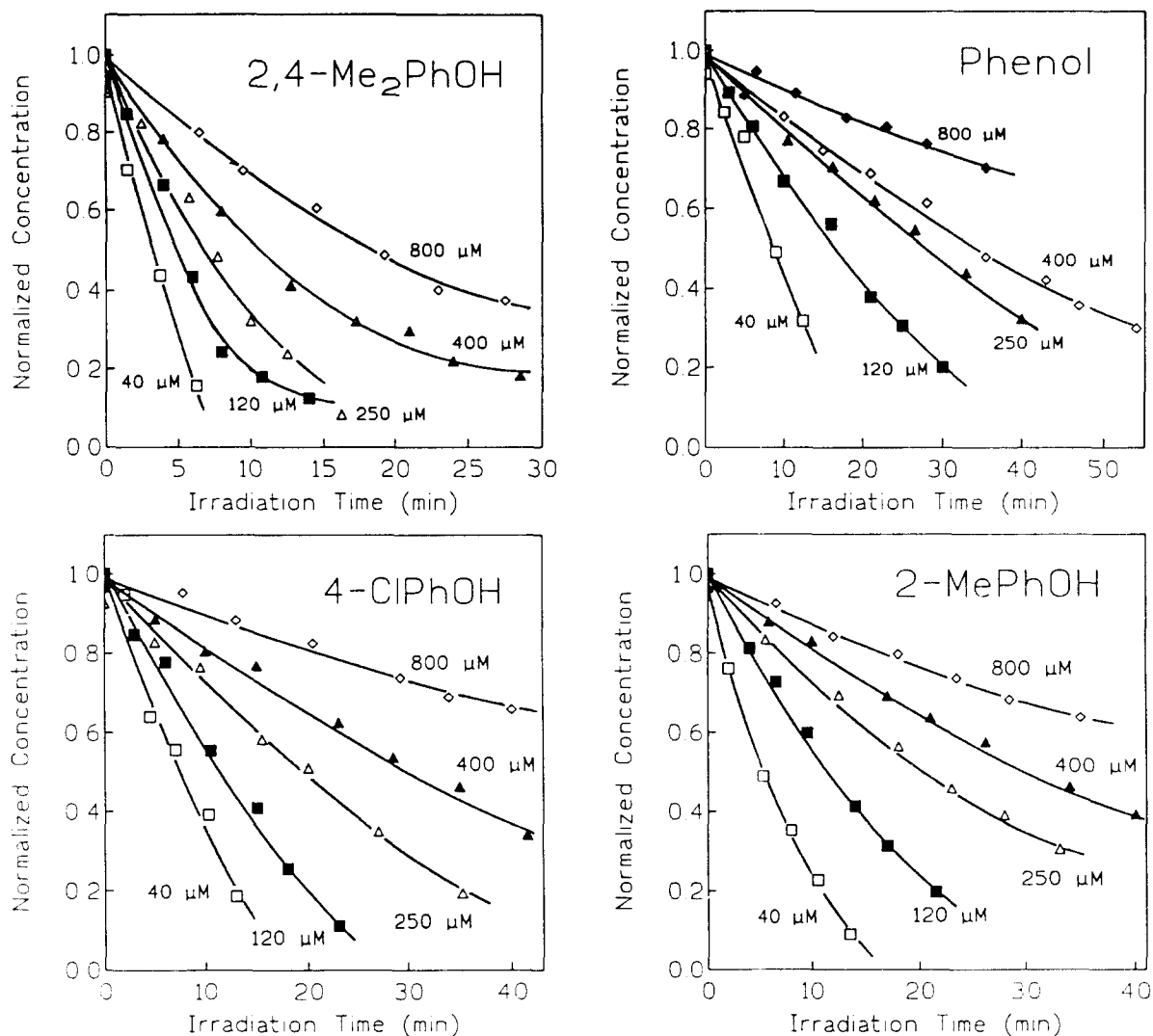
Fig. 6. Plots of the normalized concentration as a function of irradiation time for the photodegradation of phenol, 2-methylphenol, 2,4-dimethylphenol and 4-chlorophenol at five initial substrate concentrations 40, 120, 250, 400 and 800 μmol l^{-1} (reactor, 50 ml bottle; [TiO$_2$] = 2 g l^{-1}; pH 3.0).

into play and the rates ultimately scale with I_0 [34,39]. Plots of initial rates vs. light intensity for the four phenolic substrates are presented in Fig. 8. Initial rates increased with increasing light intensity and its dependences for phenol, 2-methylphenol and 4-chlorophenol are nearly identical within experimental error.

3.3. Relative photonic efficiencies

The notion of relative photonic efficiencies ζ_r was introduced above in which the effects of reactor geometry, light source and photocatalyst properties are fixed in assessing ζ for phenol and ζ for the test molecules [10].

A method to determine photon efficiencies is to relate the initial rate of substrate degradation with the rate of incident photons reaching inside the front window of the reactor. When the photonic efficiency ζ for the test substrates and for the standard secondary actinometer (here phenol) are obtained under identical experimental conditions there is no

need to measure the photon flux, although it should still be reported when experimentally feasible (certain reactor geometries may preclude such measurements). Thus

$$\zeta_r = \frac{\text{rate of disappearance of substrate}}{\text{rate of disappearance of phenol}} \qquad (6)$$

where both (initial) rates are obtained under the exact same conditions.

Ideally, ζ_r values should not depend on light intensity and reactor geometry, and on such other parameters as pH, photocatalyst concentration, substrate concentration and temperature. We now examine the influence of each of these factors on ζ_r.

3.3.1. Light intensity dependence

The effect of light intensity on relative photonic efficiencies of 2-methylphenol, 2,4-dimethylphenol and 4-chlorophenol is illustrated in Fig. 9; 100% refers to about 190 mW
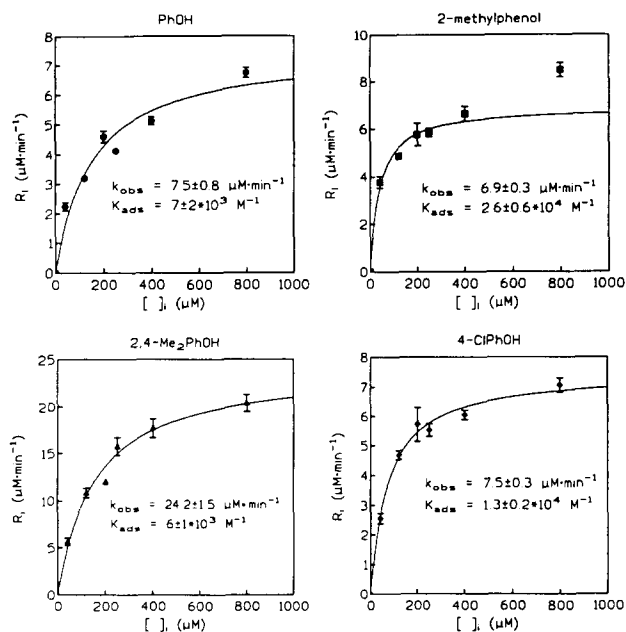
Fig. 7. Plots of initial rates vs. initial concentration for phenol, 2-methylphenol, 2,4-dimethylphenol and 4-chlorophenol at five initial substrate concentrations 40, 120, 250, 400 and 800 μmol l^{-1} (reactor, 50 ml bottle; [TiO$_2$] = 2 g l^{-1}; pH 3.0). (The point at 800 μmol l^{-1} for 2-methylphenol was not used.)
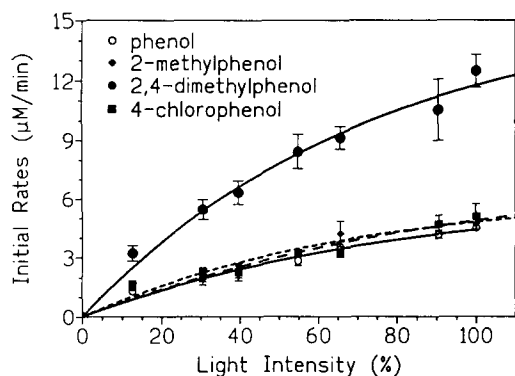

Fig. 8. Plots of initial rates vs. percentage light intensity for phenol, 2-methylphenol, 4-chlorophenol and 2,4-dimethylphenol (reactor, 50 ml bottle; [TiO$_2$] = 2 g l^{-1}; [reactant]$_i$ $\approx$ 20 mg l^{-1}; pH 3.0; 100% is equivalent to 190 mW cm^{-2}).

cm^{-2}. The efficiencies ζ_r for 2-methylphenol, 2,4-dimethylphenol and 4-chlorophenol are independent of light intensity.

3.3.2. Reactor geometry effect

Plots of ζ_r for three reactor geometries are shown in Fig. 10 for the three test substrates. The reactors were a bottle, a round-bottomed flask and a rectangular reactor with flat parallel windows. The ζ_r are nearly independent of reactor geometry.

3.3.3. pH dependence

The effect of initial pH (measured prior to addition of TiO$_2$) on the photodegradation rates was small for 4-chlorophenol and 2,4-dimethylphenol in the pH range 3–6 (Fig.

11). Relative photonic efficiencies ζ_r decrease somewhat with increase in pH, particularly so for 2,4-dimethylphenol.

3.3.4. Effect of TiO$_2$ concentration

The initial rates of photodegradation of 2-methylphenol, 2,4-dimethylphenol and 4-chlorophenol decreased slightly on going from 2 to 0.2 g l^{-1} (Table 1). However, ζ_r shows no dependence at various TiO$_2$ loadings (Fig. 12).

3.3.5. Effect of initial substrate concentration

Relative photonic efficiencies of 2-methylphenol and 4-chlorophenol display little dependence on initial concentration of substrate (Fig. 13). 2,4-Dimethylphenol, however, displays a greater dependence on its initial concentration.
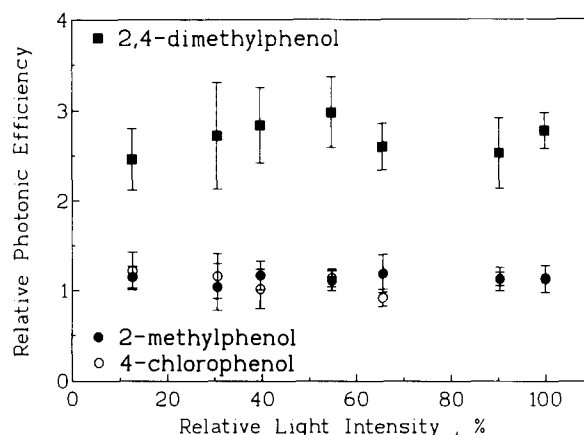

Fig. 9. Relative photonic efficiencies ζ_r determined for the disappearance of 2-methylphenol, 2,4-dimethylphenol and 4-chlorophenol at various light intensities relative to the disappearance of phenol under otherwise identical experimental conditions (reactor, 50 ml bottle; [TiO$_2$] = 2 g l^{-1}; [reactant]$_i$ $\approx$ 20 mg l^{-1}; pH 3.0; 100% is equivalent to 190 mW cm^{-2}).
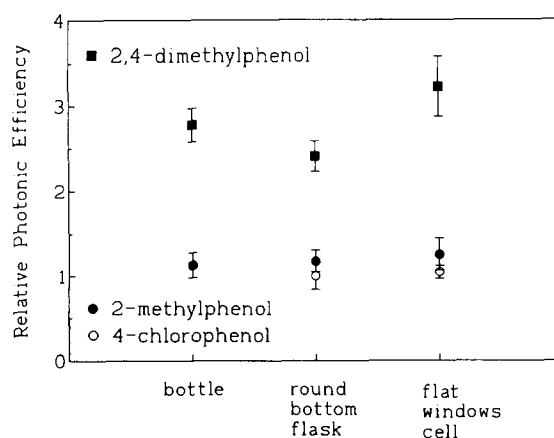

Fig. 10. Relative photonic efficiencies ζ_r determined for the disappearance of 2-methylphenol, 2,4-dimethylphenol and 4-chlorophenol in three reactor geometries: bottle, round-bottomed flask and rectangular with parallel flat windows relative to the photodegradation of phenol under identical experimental conditions ([TiO$_2$] = 2 g l^{-1}; [reactant]$_i$ $\approx$ 20 mg l^{-1}; pH 3.0).
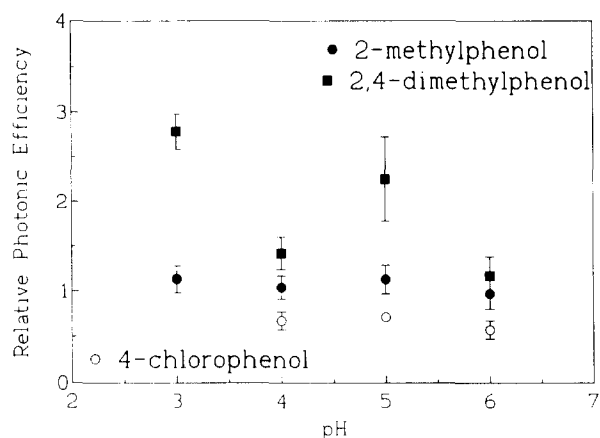
Fig. 11. Relative photonic efficiencies ζ_r determined for the disappearance of 2-methylphenol, 2,4-dimethylphenol and 4-chlorophenol at four pH values 3, 4, 5 and 6 relative to the photodegradation of phenol under identical experimental conditions (reactor, 50 ml bottle; $[TiO_2] = 2$ g l^{-1}; [substrate]$_i \approx 20$ mg l^{-1}).

Table 1
Effect of TiO_2 concentration on initial rate of photodegradation for the four phenolic compounds (reactor, 50 ml bottle; [substrate]$_i \approx 20$ mg l^{-1}; pH 3.0)

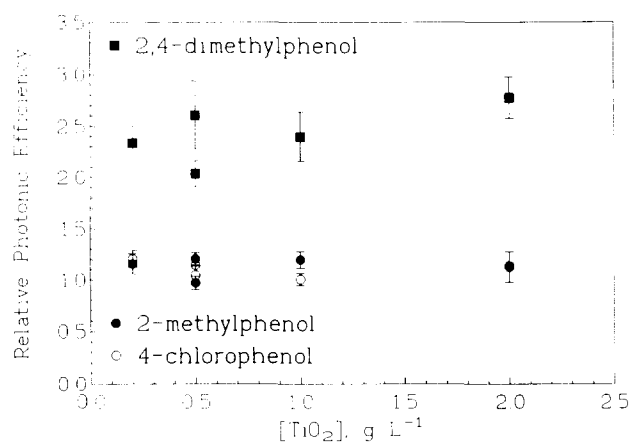| [TiO$_2$] (g l^{-1})	Initial rate (μmol l^{-1} min^{-1})			
	PhOH	2-MePhOH	2,4-Me$_2$PhOH	4-ClPhOH
2.0	4.5 ± 0.1	4.7 ± 0.1	12.5 ± 0.8	5.1 ± 0.6
1.0	4.1 ± 0.2	4.9 ± 0.3	9.9 ± 0.9	4.1 ± 0.2
0.5	3.1 ± 0.1	3.8 ± 0.1	8.2 ± 1.0	3.6 ± 0.1
0.5	4.1 ± 0.2	4.0 ± 0.2	8.3 ± 0.2	4.3 ± 0.3
0.2	3.5 ± 0.1	4.1 ± 0.3	8.2 ± 0.5	4.3 ± 0.2

Fig. 12. Relative photonic efficiencies ζ_r determined for the disappearance of 2-methylphenol, 2,4-dimethylphenol and 4-chlorophenol at four TiO_2 concentrations 0.2, 0.5, 1 and 2 g l^{-1} relative to the photodegradation of phenol under the same experimental conditions (reactor, 50 ml bottle; [reactant]$_i \approx 20$ mg l^{-1}; pH 3.0).

3.3.6. Effect of temperature

Relative photonic efficiencies ζ_r increased significantly at the higher temperatures (Fig. 14), because of different temperature dependences of the rates for each substrate relative to that of phenol.

3.3.7. Overall influence of all factors

It is important to obtain an overall view of how relative photonic efficiencies change with variations in various factors. Also we need to know what parameters should be specified when reporting ζ_r values.

Average values of ζ_r are illustrated in Fig. 15 and reported in Table 2; they are 1.1 ± 0.1 for 2-methylphenol, 2.6 ± 0.3 for dimethylphenol and 1.1 ± 0.1 for 4-chlorophenol. The results demonstrate the validity and the feasibility of the method proposed and also indicate the magnitude of the errors (one standard deviation), reasonable even by photochemical standards. Fig. 15 also illustrates the data used to estimate ζ_r under various conditions of light intensities, reactor geometries, initial pHs and TiO_2 concentrations. For 4-chlorophenol, ζ_r at pH 4, 5 and 6 were not used in the calculation of the average values. Note that the data for the initial substrate concentrations and for the different temperatures were not used.
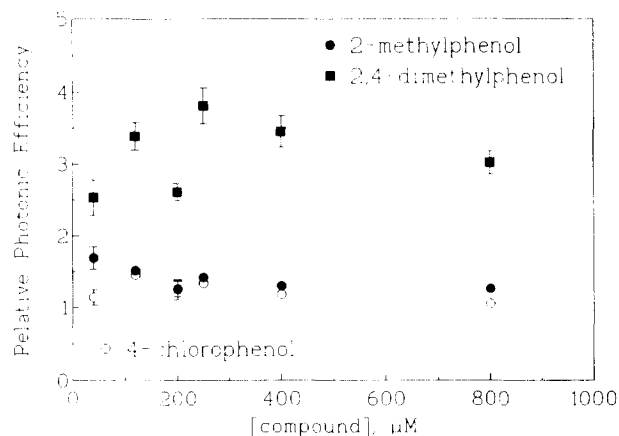

Fig. 13. Relative photonic efficiencies ζ_r determined for the disappearance of 2-methylphenol, 2,4-dimethylphenol and 4-chlorophenol at five initial substrate concentrations 40, 120, 200, 250, 400 and 800 μmol l^{-1} relative to the photodegradation of phenol under the same experimental conditions (reactor, 50 ml bottle; $[TiO_2] = 2$ g l^{-1}; pH 3.0).

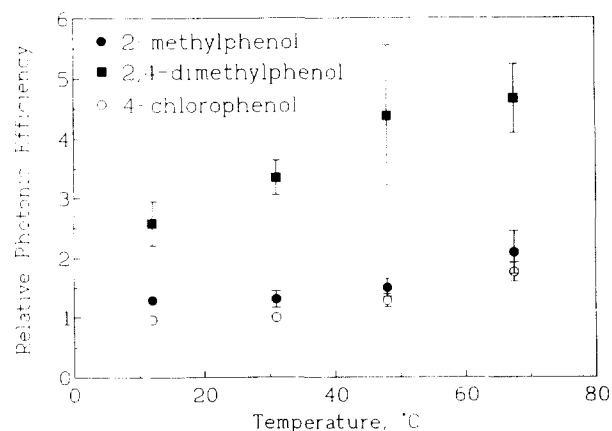Fig. 14. Relative photonic efficiencies ζ_r determined for the disappearance of 2-methylphenol, 2,4-dimethylphenol and 4-chlorophenol at four temperatures 12.0 ± 0.5, 31.0 ± 0.5, $d8.0 \pm 0.5$ and 67.5 ± 0.5 °C relative to the photodegradation of phenol under the same conditions (reactor, 50 ml bottle; $[TiO_2] = 2$ g l^{-1}; [substrate]$_i \approx 20$ mg l^{-1}; pH 3.0).
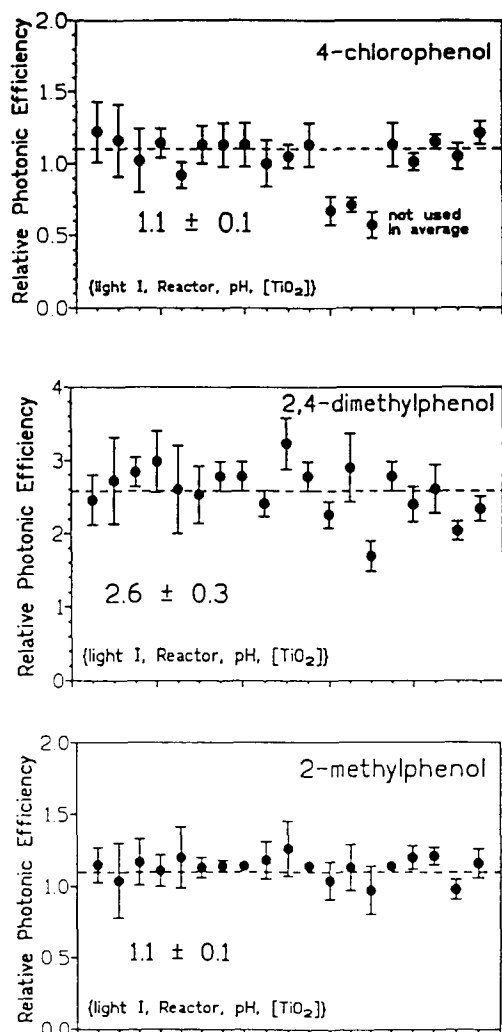
Fig. 15. Relative photonic efficiencies for 4-chlorophenol, 2,4-dimethylphenol and 2-methylphenol showing the values used to calculate averages; this includes only the effects of light intensity, reactor geometry, pH and concentration of titania ([substrate]$_i \approx$ 20 mg l^{-1}).

Table 2 also reports the relative photonic efficiencies obtained in this study for the three substrates under other conditions. We conclude that temperature, initial substrate concentration and probably also the initial pH should be cited when reporting ζ_r.

3.4. Usefulness of relative photonic efficiencies

3.4.1. ζ_r for phenolic substrates

Relative photonic efficiencies of a series of phenolic substrates are reported in Table 3 for a specified set of conditions ($C_0 = 200$ μmol l^{-1}; pH 3.0; [TiO$_2$] = 2 g l^{-1}; ambient temperature). All the efficiencies are greater than unity, indicating that the initial photocatalyzed oxidative degradations of the test substrates are more efficient than for phenol. It would appear that the substituents on the phenol provide a more efficient path for oxidation.

The ζ_r data show that the presence of one or two chloro groups on the phenol molecule has little effect on the initial

Table 2
Relative photonic efficiencies for the three phenolic substrates under various conditions (relative to phenol)

Parameter changed	Relative photonic efficiency ζ_r		
	2-Methylphenol	2,4-Dimethylphenol	4-Chlorophenol
Light intensity (%) [a]			
12.6	1.15 ± 0.12	2.46 ± 0.34	1.22 ± 0.21
30.6	1.04 ± 0.26	2.72 ± 0.59	1.16 ± 0.25
39.7	1.17 ± 0.16	2.84 ± 0.42	1.02 ± 0.22
54.8	1.11 ± 0.11	2.98 ± 0.39	1.14 ± 0.10
65.6	1.20 ± 0.21	2.60 ± 0.26	0.92 ± 0.09
90.4	1.13 ± 0.07	2.53 ± 0.39	1.13 ± 0.13
100	1.14 ± 0.04	2.78 ± 0.20	1.13 ± 0.15
Reactor geometry [b]			
Bottle	1.14 ± 0.04	2.78 ± 0.20	1.13 ± 0.15
Round-bottomed flask	1.18 ± 0.13	2.41 ± 0.18	1.00 ± 0.16
Flat windows	1.26 ± 0.19	3.23 ± 0.35	1.05 ± 0.08
Effect of pH [c]			
3.0	1.14 ± 0.02	2.78 ± 0.20	1.13 ± 0.15
4.0	1.04 ± 0.13	1.42 ± 0.18	0.67 ± 0.10
5.0	1.13 ± 0.16	2.25 ± 0.47	0.71 ± 0.05
6.0	0.97 ± 0.17	1.17 ± 0.21	0.57 ± 0.09
TiO$_2$ loading [d] (g l^{-1})			
2.0	1.14 ± 0.04	2.78 ± 0.20	1.13 ± 0.15
1.0	1.20 ± 0.08	2.40 ± 0.24	1.01 ± 0.06
0.5	1.21 ± 0.06	2.61 ± 0.33	1.15 ± 0.05
0.5	0.98 ± 0.07	2.04 ± 0.13	1.05 ± 0.09
0.2	1.16 ± 0.10	2.34 ± 0.17	1.21 ± 0.08
Phenolic substrate concentration [e] (μM)			
40	1.69 ± 0.16	2.53 ± 0.25	1.14 ± 0.11
120	1.52 ± 0.05	3.38 ± 0.19	1.46 ± 0.06
200	1.26 ± 0.11	2.61 ± 0.12	1.25 ± 0.14
250	1.42 ± 0.06	3.81 ± 0.25	1.34 ± 0.06
400	1.30 ± 0.07	3.45 ± 0.22	1.18 ± 0.05
800	1.26 ± 0.06	3.02 ± 0.16	1.05 ± 0.05
Temperature [f] (°C)			
12.0	1.29 ± 0.05	2.58 ± 0.37	0.96 ± 0.06
31.0	1.31 ± 0.14	3.35 ± 0.29	1.00 ± 0.06
48.0	1.50 ± 0.15	4.38 ± 1.17	1.28 ± 0.11
67.5	2.09 ± 0.36	4.67 ± 0.57	1.76 ± 0.16

[a] pH 3; TiO$_2$ loading, 2.0 g l^{-1}; substrate concentration, 20 mg l^{-1}; ambient temperature. Note 100% light intensity is equivalent to about 190 mW cm^{-2}.
[b] pH 3; light intensity, 100%; TiO$_2$ loading, 2.0 g l^{-1}; substrate concentration, 20 mg l^{-1}; ambient temperature.
[c] Light intensity, TiO$_2$ loading, 2.0 g l^{-1}; substrate concentration, 20 mg l^{-1}; ambient temperature.
[d] pH 3; light intensity, 100%; substrate concentration, 20 mg l^{-1}; ambient temperature.
[e] pH 3; light intensity, 100%; TiO$_2$ loading, 2.0 g l^{-1}; ambient temperature.
[f] pH 3; light intensity, 100%; TiO$_2$ loading, 2.0 g l^{-1}; substrate concentration, 20 mg l^{-1}.

oxidation. By contrast, for methylated phenols we observe efficiencies greater than for phenol or chlorophenols. Alkylation increased ζ_r, and this increase seems to depend on the position of the alkyl groups on the phenol. The highest ζ_r amongst the methylphenols is seen when the methyl group is *para* to OH. The highest efficiency amongst the dimethylphenols is shown by methyl groups when both are in the ortho positions, followed by the species with one *ortho* and one

Table 3

Relative photonic efficiencies for various phenolic substrates using phenol as the standard reference (initial concentration, about 200 μmol l^{-1}; [TiO$_2$] = 2 g l^{-1}; pH 3.0)

Substrate	Relative photonic efficiency
Phenol	1.00
2-methylphenol	1.2 ± 0.1
3-methylphenol	1.3 ± 0.1
4-methylphenol	1.6 ± 0.1
2,3-dimethylphenol	2.0 ± 0.2
2,4-dimethylphenol	2.7 ± 0.1
2,5-dimethylphenol	2.3 ± 0.1
2,6-dimethylphenol	3.0 ± 0.2
3,4-dimethylphenol	2.5 ± 0.2
3,5-dimethylphenol	1.6 ± 0.2
2,3,5-trimethylphenol	2.8 ± 0.4
2-chlorophenol	1.2 ± 0.1
3-chlorophenol	1.0 ± 0.1
4-chlorophenol	1.2 ± 0.1
2,4-dichlorophenol	1.0 ± 0.1

Table 4

Relative photonic efficiencies for the photodegradation of phenol in the presence of various TiO$_2$ sources relative to the photodegradation of phenol in the presence of Degussa P25 titania (initial concentrations, about μmol l^{-1}; [TiO$_2$] = 2 g l^{-1}; pH 3.0)

Source of TiO$_2$	Relative photonic efficiency
Degussa P25 (A)	1.00 ± 0.06
Degussa P25 (B)	0.99 ± 0.06
Degussa P25 (C)	0.99 ± 0.06
Baker & Adamson	0.38 ± 0.02
Degussa P25 (A)	1.00 ± 0.05
Tioxide	1.94 ± 0.08
Sargent–Welch	2.05 ± 0.11
Fluka AG	2.21 ± 0.16
Sachtleben Chemie (Hombikat UV-100)	0.25 ± 0.02

para to OH. The lowest efficiency amongst the dimethylphenols occurs when both methyl groups are in the *meta* positions.

Methyl groups are weak electron-donating substituents so that the electron density over the aromatic ring nucleus should be increased somewhat. This should facilitate the attack by electrophilic species. Indeed, the Hammett coefficient σ has been used among the several possible descriptors for the photocatalytic degradability of chlorophenols and substituted methoxybenzenes (anisoles) [35,36]. Also, the position of the OH substituent may explain the highest ζ_r found for phenol substituted at the *para* and/or *ortho* position, although σ is not the only descriptor to be considered to interpret the results fully.

3.4.2. ζ_r for different photocatalyst specimens

The ζ_r concept can also be applied in heterogeneous photocatalysis to standardize the activity of various photocata-
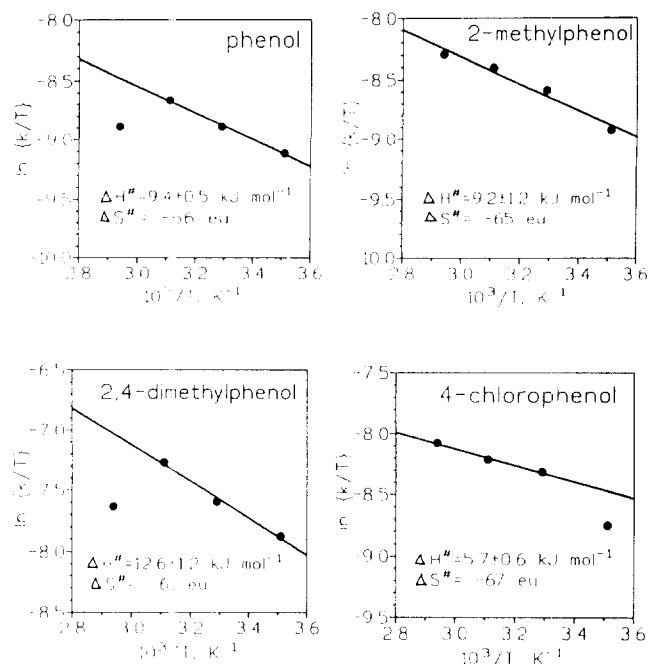

Fig. 16. Eyring plots of ln(k/T) vs. $10^3/T$ for the photodegradations of 2-methylphenol, 2,4-dimethylphenol and 4-chlorophenol. The four temperatures were 12.0 ± 0.5, 31.0 ± 0.5, 48.0 ± 0.5 and 67.5 ± 0.5 °C ([TiO$_2$] = 2 g l^{-1}; [substrate]$_i$ = 20 mg l^{-1}; pH 3.0).

lysts from different sources for a given process. Table 4 summarizes relative photonic efficiencies for the photooxidation of phenol in the presence of various TiO$_2$ materials (all relative to Degussa P25-A specimen). Three different batches of Degussa P25 TiO$_2$ (all mostly in the anatase form) gave, within experimental errors, identical ζ_r which illustrates the batch to batch consistency from the same source. Titania from Baker & Adamson (of unknown form) gave ζ_r lower than unity; it is less efficient than Degussa P25 titania. By contrast, titania specimens from Tioxide (anatase form), Sargent–Welch (of unknown form) and Fluka (anatase) gave ζ_r greater than unity. They indicate that the initial oxidative degradation process for phenol is more effective than with Degussa P25 titania. In this regard, we noted earlier that additional intermediates, in greater quantities, were detected with Tioxide, Sargent–Welch and Fluka titania samples than with Degussa P25. The intermediates are often themselves pollutants so that the mineralization of total organic carbon becomes of greatest importance in any water treatment process. The Hombikat UV-100 TiO$_2$ sample (100% anatase; Sachtleben Chemie, Germany) is about four times less efficient than the Degussa P25 TiO$_2$ standard with respect to oxidation of phenol and to its complete mineralization to CO$_2$ and water. Further details of this latter study have been presented elsewhere [40].

3.5. Kinetic considerations

3.5.1. Activation parameters

The temperature dependence study affords phenomenological activation parameters that might permit some inferences regarding overall energies of activation. Fig. 16 shows Eyring

plots of $\ln(k_{obs}/T)$ vs. $10^3/T$ for phenol, 2-methylphenol, 2,4-dimethylphenol and 4-chlorophenol. The rates seem to decrease at the highest temperature examined. The rates of processes occurring in a semiconductor shown in Fig. 1 will no doubt have different temperature dependences, some of which, for example, adsorption and desorption phenomena are known to be temperature-dependent processes [41]. In addition, at the higher temperatures other processes (e.g. electron–hole recombination which is to some extent distance dependent) may influence the overall observed rate constant. Bahnemann et al. [14] reported a decrease in the rates of disappearance of chloroform with increasing temperature at high light fluxes over the entire temperature range 15–75 °C.

Enthalpies $\Delta H^{\neq}$ and entropies $\Delta S^{\neq}$ of activation are reported in Fig. 16. The data points at 67.5 °C were not used in the calculations of these parameters in some cases. For phenol, $\Delta H^{\neq} = 9.4 \pm 0.5$ kJ mol^{-1} (identical with $\Delta H^{\neq}$ for 2-MePhOH; 9.2 ± 1.2 kJ mol^{-1}) in the temperature range 12–48 °C in line with the activation energy ($E_a \approx 7$ kJ mol^{-1}) or about 10 kJ mol^{-1} reported previously in a similar temperature range [30]. A lower value ($E_a \approx 2.6 \pm 0.5$ kJ mol^{-1}) was reported by others in the temperature range 20–60 °C [42]. The enthalpy of activation of 4-chlorophenol is $\Delta H^{\neq} = 5.7 \pm 0.6$ kJ mol^{-1} and $E_a = 3.2 \pm 0.6$ kJ mol^{-1} also in line with $E_a \approx 5.5$ kJ mol^{-1} reported earlier for a comparable temperature range [38]. For 2,4-dimethylphenol, $\Delta H^{\neq} = 12.6 \pm 1.2$ kJ mol^{-1} and $E_a \approx 10.1 \pm 1.2$ kJ mol^{-1}; for the analogous 3,4-dimethylphenol in the temperature range 5–60 °C, $E_a \approx 8.8 \pm 0.8$ kJ mol^{-1} [34]. By comparison, comparable activation energies were reported for the photodegradation of salicylic acid ($E_a \approx 11.0 \pm 0.8$ kJ mol^{-1}; temperature range, about 20–50 °C [43]) and for dichloroacetic acid ($E_a \approx 16.2$ kJ mol^{-1}; temperature range unspecified [44]).

The above activation energies compare with activation energies found for reactions of hydroxyl radicals with formate and 2-propanol in homogeneous phase ($E_a \approx 5$–10 kJ mol^{-1} [45]). This observation would appear to support mechanism (ii) that implicates $\equiv$Ti^{IV}–$\cdot$OH radicals as the oxidizing entities in heterogeneous photocatalyzed oxidations. However, we hasten to point out that this comparison may be entirely fortuitous since there are a plethora of steps that may be photon activated and/or thermally activated. Nevertheless, the near congruence of the energies of activation is interesting. The entropies of activation for the oxidative degradation of the four substrates are large and negative ($\Delta S^{\neq} \approx -61$ to -67 eu) and, while the mechanistic details are not forthcoming owing to the complexity of events, it is nevertheless comforting to note that such entropies are consistent with the notion, which has evolved from other studies, that the photo-oxidation is a surface-occurring reaction.

4. Conclusions

The use of relative photonic efficiencies, ζ_r, renders comparison of process efficiencies (relative to phenol, in the present case) between studies carried out in other laboratories possible because ζ_r is basically independent of light intensity, reactor geometry and TiO$_2$ concentration for a given TiO$_2$ sample. However, ζ_r depends on the initial concentration of substrate, on temperature and, apparently to a lesser degree, on pH. These relative photonic efficiencies can be used to compare photon efficiencies of various organic substrates and to determine which one is transformed most efficiently. Note that this study examined only phenolic substrates to test the generality of the method; in future, other types of organic substrate should be explored.

Relative photonic efficiency based on initial rates of degradation illustrates only one aspect of photodegradations and is useful to also compare distinct photocatalyst materials for water treatment purposes. The possibility of efficiencies based on the disappearance of total organic carbon, or CO$_2$ formation would be more informative in a practical sense and should be investigated [40]. Moreover, ζ_r could be used to check batch-to-batch reproducibility for a given photocatalyst material and ultimately to estimate the photochemically defined quantum yield, once an acceptable and unambiguous method(s) has been found to describe the number of absorbed photons.

Finally, it is noteworthy that the parameters that appear to influence ζ_r are those that may have an effect on the adsorption–desorption properties of the organic substance on titania (e.g. concentration of the organic substrate, temperature and pH) whereas those parameters that have little influence, if any, on adsorption–desorption (e.g. reactor geometry, light intensity and titania concentration) show no variations in ζ_r.

References

[1] D.F. Ollis, E. Pelizzetti and N. Serpone, in N. Serpone and E. Pelizzetti (eds.) Photocatalysis — Fundamentals and Applications, Wiley, New York, 1989, pp. 603–637.

[2] D.W. Bahnemann, J. Cunningham, M.A. Fox, E. Pelizzetti, P. Pichat and N. Serpone, in G.R. Helz, R.G. Zepp and D.G. Crosby (eds.), Aquatic and Surface Photochemistry. Lewis Publishers, Boca Raton, FL, 1994, pp. 261–316.

[3] R. Terzian, N. Serpone, C. Minero and E. Pelizzetti, J. Catal., 128 (1991) 352.

[4] D.F. Ollis, E. Pelizzetti and N. Serpone, Environ. Sci. Technol., 25 (1991) 1523.

[5] D.F. Ollis, Environ. Sci. Technol., 19 (1985) 480.

[6] (a) J.C. D'Oliveira, G. Al-Sayyed and P. Pichat, *Environ. Sci. Technol.*, 24 (1990) 990.
(b) S. Doherty, C. Guillard and P. Pichat, *J. Chem. Soc. Faraday Trans.*, 91 (1995) 1853, and references cited therein.

[7] E. Pelizzetti, M. Barbeni, E. Pramauro, N. Serpone, E. Borgarello, M.A. Jamieson and H. Hidaka, *Chim. Ind. (Milano)*, 67 (1985) 623.

[8] J.R. Bolton and S.R. Cater, in G.R. Helz, R.G. Zepp and D.G. Crosby (eds.), *Aquatic and Surface Photochemistry*, Lewis Publishers, Boca Raton, FL, 1994, pp. 467–490.

[9] O. Legrini, E. Oliveros and A.M. Braun, *Chem. Rev.*, 93 (1993) 671.

[10] N. Serpone, R. Terzian, D. Lawless, P. Kennepohl and G. Sauve, *J. Photochem. Photobiol. A: Chem.*, 73 (1993) 11.

[11] F. Sabin, T. Türk and A. Vogler, *J. Photochem. Photobiol. A: Chem.*, 63 (1992) 99.

[12] J.G. Calvert and J.N. Pitts, Jr., *Photochemistry*, Wiley, New York, 1966, pp. 780 ff.

[13] A.M. Braun, M.-T. Maurette and E. Oliveros, *Photochemical Technology* (translated from *Technologies Photochimiques* by D.F. Ollis and N. Serpone), Wiley, Chichester, West Sussex, 1991, Chapter 2.

[14] D.W. Bahnemann, D. Bockelmann and R. Goslich, *Sol. Energy Mater.*, 24 (1991) 564.

[15] P. Pichat, in M. Schiavello (ed.), *Photochemistry, Photocatalysis and Photoreactors*, Reidel, Dordrecht, 1985, pp. 425–455.

[16] L.P. Childs and D.F. Ollis, *J. Catal.*, 66 (1980) 383.

[17] M. Schiavello, V. Augugliaro and L. Palmisano, *J. Catal.*, 127 (1991) 332.

[18] V. Augugliaro, L. Palmisano and M. Schiavello, *AIChE J.*, 37 (1991) 1096.

[19] L. Palmisano, V. Augugliaro, R. Campostrini and M. Schiavello, *J. Catal.*, 143 (1993) 149.

[20] M.I. Cabrera, O.M. Alfano and A.E. Cassano, *Ind. Eng. Chem. Res.*, 33 (1994) 3031.

[21] D.H. Everett, *Basic Principles of Colloid Science*, Royal Society of Chemistry, London, 1988.

[22] I. Rosenberg, J.R. Brock and A. Heller, *J. Phys. Chem.*, 96 (1992) 3423.

[23] R.C. Weast (ed.), *CRC Handbook of Chemistry and Physics*, Vol. 51, Chemical Rubber Co., Cleveland, OH, 1970–1971.

[24] L. Sun and J.R. Bolton, *J. Phys. Chem.*, submitted for publication.

[25] N. Serpone, E. Pelizzetti and H. Hidaka, in Z.W. Tian and Y. Cao (eds.), *Photochemical and Photoelectrochemical Conversion and Storage of Solar Energy*, International Academic Publishers, Beijing, 1993, pp. 33–74.

[26] M. Boudart and G. Djega-Mariadassou, *Kinetics of Heterogeneous Catalytic Reactions*, Princeton University Press, Princeton, NJ, 1984.

[27] N. Serpone, D. Lawless, R. Khairutdinov and E. Pelizzetti, *J. Phys. Chem.*, 99 (1995) 16655.

[28] D. Lawless, *Ph.D. Thesis*, Concordia University, Montreal, January 1993.

[29] D.E. Skinner, D.P. Colombo, Jr., J.J. Cavalieri and R.M. Bowman, *J. Phys. Chem.*, 99 (1995) 7853.

[30] K. Okamoto, Y. Yamamoto, H. Tanaka and A. Itaya, *Bull. Chem. Soc. Jpn.*, 58 (1985) 2023.

[31] M.A. Fox, R.B. Draper, M. Dulay and K. O'Shea, in E. Pelizzetti and M. Schiavello (eds.), *Photochemical Conversion and Storage of Solar Energy*, Kluwer, Dordrecht, 1991, pp. 323–335.

[32] U. Stafford, K.A. Gray and P.V. Kamat, *J. Phys. Chem.*, 98 (1994) 6343.

[33] A. Mills, S. Morris and R. Davies, *J. Photochem. Photobiol. A: Chem.*, 70 (1993) 183.

[34] (a) R. Terzian, *Ph.D. Thesis*, Concordia University, Montreal, January 1993.
(b) R. Terzian and N. Serpone, *J. Photochem. Photobiol. A: Chem.*, 89 (1995) 163.

[35] N. Jaffrezic-Renault, P. Pichat, A. Foissy and R. Mercier, *J. Phys. Chem.*, 90 (1986) 2733.

[36] K.Ch. Akratopulu, C. Kordulis and A. Lycourghiolis, *J. Chem. Soc., Faraday Trans.*, 86 (1990) 3437.

[37] M. Barbeni, E. Pramauro, E. Pelizzetti, M. Grätzel and N. Serpone, *Nouv. J. Chim.*, 8 (1984) 550.

[38] G. Al-Sayyed, J.-C. D'Oliveira and P. Pichat, *J. Photochem. Photobiol. A: Chem.*, 58 (1991) 99.

[39] C.S. Turchi and D.F. Ollis, *J. Catal.*, 122 (1990) 178.

[40] H. Tahiri, N. Serpone and P. Pichat, *J. Photochem. Photobiol. A: Chem.*, in press.

[41] W. Mu, J.-M. Herrmann and P. Pichat, *Catal. Lett.*, 3 (1989) 73.

[42] E. Pelizzetti, C. Minero, E. Borgarello, L. Tinucci and N. Serpone, *Langmuir*, 9 (1993) 2995.

[43] R.W. Matthews, *J. Phys. Chem.*, 91 (1987) 3328.

[44] D.W. Bahnemann, D. Bockelmann, R. Goslich, M. Hilgendorf and D. Weichgrebe, in D.F. Ollis and H. Al-Ekabi (eds.), *Photocatalytic Purification and Treatment of Water and Air*, Elsevier, Amsterdam, 1992, pp. 301–319.

[45] A.J. Elliott and A.S. Simsons, *Radiat. Phys. Chem.*, 24 (1984) 229.